Use of a Plasma Focus Device to study pulsed X-rays effects on Peripheral Blood Lymphocytes: Analysis of Chromosome Aberrations

Authors: Valentina Verdejo[a], Analía Radl[a], Joan-Francesc Barquinero[b], Jalaj Jain[c], Sergio Davis[c,d], Cristian Pavez[c,d], Leopoldo Soto[c,d] and José Moreno[c,d]*

Affiliations:

[a] Laboratorio Dosimetría Citogenética, Comisión Chilena de Energía Nuclear, Casilla 188-D, 7600713 Santiago, Chile

[b] Departamento de Biología Animal, Biología Vegetal y Ecología, Universitat Autònoma de Barcelona, 08193 Barcelona, Spain

[c] Research Center on the Intersection in Physics of Plasmas, Matter and Complexity, P2mc, Comisión Chilena de Energía Nuclear, Casilla 188-D, 7600713 Santiago, Chile

[d] Universidad Andrés Bello, Departamento de Ciencias Físicas, Republica 220, Santiago-8370035, Chile

*Corresponding author: José Moreno. E:mail: jose.moreno@cchen.cl. Phone: +562 2364 6243

Journal of Applied Physics

AIP Publishing

ABSTRACT

X-ray pulses (Full Width at Half Maximum ~ 90 ns, dose rate ~ 10^7 Gy·sec^{-1}) were used to irradiate a monolayer of peripheral blood mononucleated cells (PBMCs) using the PF-2kJ kilojoule plasma focus device. Four different exposure conditions were evaluated using 5, 10, 20, and 40 pulses, with the mean dose measured by TLD-100 being 0.12 ±0.02 mGy, 0.14±0.03 mGy, 0.22±0.06 mGy, and 0.47±0.09 mGy, respectively. Cytogenetic analysis showed an increase in all types of chromosomal aberrations following exposure to X-ray pulses.

The distribution of dicentrics and centric rings was overdispersed after 5, 10, 20 and 40 pulses. Additionally, after 20 and 40 pulses the presence of tricentric chromosomes is detected. Chromosome aberration frequencies found in this study were always higher than the estimated frequencies of chromosome aberrations using published dose effect curves for conventional radiation sources. The overdispersion observed, the elevated Maximum Relative Biological Effectiveness, RBE_M, and the presence of tricentric chromosomes at the relatively low doses of exposure (<0.5 Gy) seems to indicate that low doses of pulsed X-rays of low energy show similar biological effects as those observed for high-LET radiation. X-rays pulses emitted by PF- 2kJ were found more efficient in inducing chromosome aberrations, even more than α particles.

Keywords: Chromosome aberrations, pulsed X-rays, peripheral blood lymphocytes, low dose, plasma focus device

1. Introduction

The development and use of pulsed radiation sources in different fields of science and industry [1-2], make it necessary to know and characterize the effects of these radiations on different types of matters. The evaluation of their biological effect is of relevance for their possible applications in radiotherapy treatments, and for radiological protection measures.

Several studies showed that the ultra-high dose-rate (UHDR) pulsed (Full Width at Half Maximum, FWHM of tens of nanoseconds, ~10^9 Gy·s^{-1}) irradiations of high energies (~ MeV) effects on biological samples are not so different from continuous-conventional (CONV) irradiation effects [3-5]. Recently, pulsed X-ray emitted from a kilojoule plasma focus device, PF-2kJ (FWHM of about 90 ns, 10^7 Gy·s^{-1}, low energy 8-10 keV), has been applied to irradiate several cancer cell lines and the obtained results showed a higher cell death in comparison to conventional X-ray source irradiation at the same doses [6]. In other studies, using plasma focus devices, the higher effects of pulsed X-rays irradiation on cancer cells have been reported [7-9]. The above mentioned research demand to continue the study in order to understand the difference on the biological effect between pulsed and conventional (continuous) radiation, analyzing different biological endpoints (cell survival, mutations and chromosome aberrations) and/or cell lines (tumor cell, stem cells, blood cells). To do so in the present work, a kilojoule plasma focus device, PF-2kJ, was used to irradiate blood lymphocyte samples. The chromosome aberrations from peripheral blood lymphocytes were analyzed, this cytogenetic biomarker is widely used in radiobiology and radioprotection for conventional radiation sources. Since a plasma focus device is used in the present work, in the following a brief of radiation emission from plasma focus devices is presented.

Plasma focus devices produce pulsed plasma and radiation pulses using transient electrical discharges. Various types of pulsed radiation are emitted from the plasma focus devices (~10-100 ns); low (~ 5-15 keV) and high-energy (> hundreds of keV X-rays) [10-15], neutrons (~ MeV) [11, 16-19], ions [11, 20-23], relativistic electrons [24], and ultra-high frequency (UHF) electromagnetic radiation [25-27]. Various schemes have been proposed to improve the performance of plasma focus devices concerning radiation emission [28-30]. Different electrode geometries; oval-shaped anode, conical top anode, and stepped anode have been tested and it was found that the conical top anode had a better performance [29-30]. The present work uses a conical top anode to get the maximum X-ray emission using hydrogen as the working gas that only produces X-rays. Among other effects induced by ionizing radiation (IR), like X-rays, the double-strand breaks in the DNA molecule are the most important. Consequences of these lesions are mutations and chromosome aberrations due to unrepair or misrepair during the cellular cycle division [31]. Dicentric chromosomes are formed by the misjoining of two broken chromosomes that carry the centromeric region of each chromosome; the formation of centric rings results from the erroneous joining of a chromosome that breaks into two arms, joining itself. In either of these cases the remaining acentric chromosome fragments also join, forming what is known as an acentric fragment [32]. These chromosome aberrations (CA) are almost exclusively induced by IR [33]. The CA frequency is also commonly used as a cytogenetic biomarker of dose exposure [34]. The analysis of this biomarker in peripheral blood lymphocytes (PBL) is considered a robust and "gold standard" biological dosimetry method and an important tool in the area of radiation protection [35-36]. Dicentric chromosomes and centric rings are the most reliable and repeatable method for comparing biological response for a wide range of doses and qualities of ionizing radiation [37].

The Relative Biological Effectiveness (RBE) is the ratio of the absorbed doses of two types of radiation that produce the same specified effect, and the Maximum Relative Biological Effectiveness (RBE_M) is the ratio of linear coefficients (α coefficient) of the dose–response curves for the radiation of interest and a reference radiation [38]. The RBE_M using chromosome aberrations as cytogenetic endpoint in PBL after IR exposure has been studied for different radiation qualities [37, 39-41]. High linear energy-transfer (high-LET) irradiations, such as neutrons and α-particles, have greater biological effectiveness than low linear energy-transfer (low-LET), like X-rays or γ-rays. However, low-energy X-rays are more biologically effective, per unit absorbed dose, than high-energy X-rays or γ-rays due to the production of lower energy secondary electrons [37, 40, 42-43]. RBE_M values have not been reported for low-dose, ultra-high dose rate and low-energy pulsed X-rays. Thus, in the present work a kilojoule plasma focus device, PF-2kJ, is adapted as an ultra-high dose rate pulsed low-energy X-rays source (8-10 keV, FWHM ~90 ns, 10^7 $Gy \cdot s^{-1}$), to evaluate the biological effectiveness using chromosome aberrations as cytogenetic biomarker in peripheral blood lymphocytes (PBL).

2. Methods

2.1. Experimental Setup.

A schematic of the kilojoule plasma focus device, PF-2kJ [23], for dose measurement and lymphocyte irradiation is shown in Figure 1. PF-2kJ (Figure 1-A) consists of a central electrode, anode, partially covered by an alumina insulator. The conical anode top geometry was proposed to have better pinching action in a PF device with ~ 2kJ energy [29], thus being used in the present work. Normally, the PF devices consist of a coaxial electrode geometry in which cathode bars symmetrically surround the central anode, unlike the present work. High X-ray emission is reported for the same device and others

without cathode bars [30,44]. The external diameter of the anode was ~24 mm and the effective length was ~ 46 mm. Electrical parameter of the PF-2kJ can be found in Jain et al. 2019 [23]. A photomultiplier tube, PMT, model Photonis XP2262B (Photonis Imaging sensors, USA) in combination with the scintillator BC-408 (Saint Gobain, USA) was mounted at a distance of ~ 82 cm in the axial direction to monitored the presence of X-ray as reference tool. A lead piece was kept at the bottom of the anode to increase the X-ray emission [7]. An array of 21 TLD-100 thermoluminescent dosimeters (RadPro, Wermelskirchen, Germany) was arranged in a petri dish (Figure 1-B) and kept over the plastic vacuum window at a distance of ~5.5 cm from the anode top. These dosimeters show linearity in the energy range keV to MeV [45-47].

Plasma focus devices emit a large amount of X-ray in the low energy range [48]. The estimated average X-ray energies (low-energy zone) emitted from the PF-2kJ are about 8-10 keV. Such estimations were based on the dosimetric measurements and HVL values [49]. Because of this, a high-density plastic vacuum window was used so that maximum X-ray transmission can take place [7].

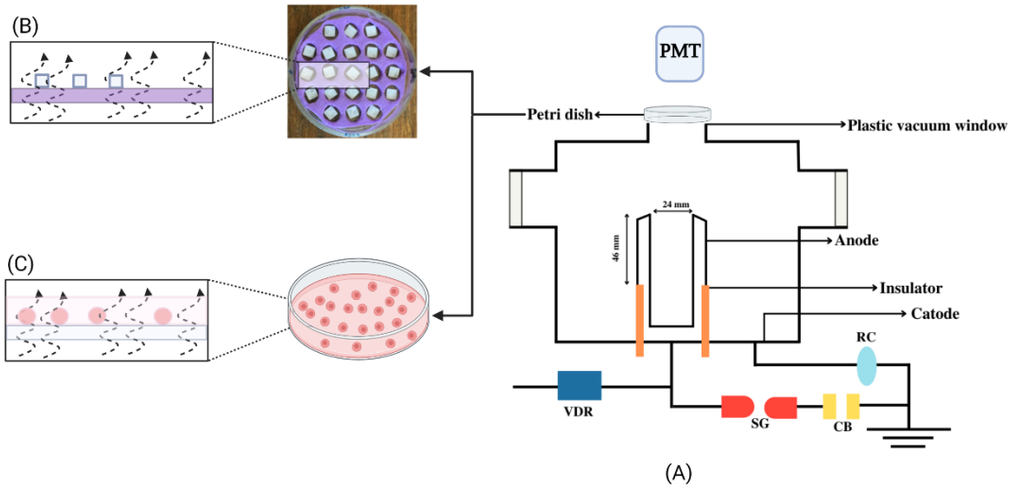

Figure 1. Experimental setup. (A) Schematic of the kilojoule plasma focus device, PF-2kJ, **PMT**: photomultiplier tube; **VDR**: resistive voltage divider, **SG**: Spark-Gap, **RC**: Rogowski coil, **CB**: capacitor bank (B) arrangement of TLD-100 dosimeters, and (C) arrangement for cell irradiation.

2.2. Isolation of Peripheral Blood Mononucleated Cells.

Peripheral blood samples from a 50-years-old male with no ionizing radiation or clastogenic exposure history were collected in heparinized tubes. Previous informed consent was obtained. The same blood donor has been used in all irradiation conditions, so that the influence of interindividual variations is eliminated.

Because of the attenuation of photon energies (8-10 keV) of this plasma focus device, irradiation assays were performed using a monolayer of human peripheral lymphocytes. For this, peripheral blood mononucleated cells (PBMCs) were separated using the density gradient method by Histopaque® 1077 (Sigma-Aldrich Company Ltd., Gillingham, United Kingdom). Three milliliters of heparinized blood were mixed 1:1 in RPMI-1640

(supplemented with L-glutamine and 25 mM HEPES; Gibco, Grand Island, New York, USA), gentled deposited onto 3 mL of Histopaque-1077 and centrifuged at 400 ×g for 30 min at room temperature. After aspirating the upper layer, the opaque interface containing PBMCs was collected into a clean 15 mL conical tube (Corning Inc., New York, USA). Cells were washed using 10 mL of RPMI-1640 medium, after centrifuging at 700 ×g for 15 min, the supernatant was discarded and cells were resuspended on 2 mL of RPMI-1640. Using a dilution of 1:10 of this cell solution, concentration was calculated by Neubauer chamber (Brand, Wertheim, Germany). PBMCs were diluted considering the maximum cell concentration to achieve a monocellular layer of cells on a 35 mm Petri dish that is $6.13 \cdot 10^6$ cell·mL^{-1}. In all irradiation conditions 2 mL of cell solution was added to Petri dish.

2.3. Irradiation Conditions

Irradiation assays were done on 35 mm polystyrene Petri dishes, uncoated and tissue culture treated (Nest, Jiangsu, China) (Figure 1-C). After the addition of the PBMCs dilution, the dishes were left undisturbed for 30 min to allow sedimentation according to the method of Virsik et al. [50]. The monolayers of cells settled on the bottom of the dishes were exposed separately to 5, 10, 20, and 40 pulses of X-ray emitted from the PF-2kJ device (FWHM ~ 90 ns, dose rate ~ 10^7 Gy·s^{-1}), two independent experiments were performed for each irradiation conditions. Additionally, an unirradiated monolayer sample was prepared to evaluate the effect of sham irradiated conditions. An array of 21 TLD-100 dosimeters in the same type of Petri dish was positioned at the anode top, to measure the doses under the same irradiation conditions.

2.4. Lymphocyte Culture and Chromosome Analysis

After irradiation, cells were collected in a 15 mL conical tube (Corning), washed with 2 mL of RPMI 1640 medium, and centrifuged 10 min to 700 ×g. The supernatant was discarded and cells were resuspended on 0.5 mL of RPMI 1640 medium. The cells were incubated at 37 °C for 2 h with 4 mL RPMI 1640 medium, supplemented with 18 % of Fetal Bovine Serum (Gibco, Grand Island, New York, USA). To stimulate lymphocyte growth Phytohemagglutinin M (Gibco, Grand Island, New York, USA) 1.8 % v/v was added. Lymphocyte cultures were done in presence of 5-Bromo-2′-deoxyuridine (0.9 % v/v) (Calbiochem, San Diego, California, USA). Since an increase in radiation dose can delay the progression of the cell cycle [51-53], and in order to obtain a sufficient number of cells for analysis, the length of culture were 48 h, 50h and 72h for 5-10, 20 and 40 pulses respectively. In all the cases, Colcemid (Gibco, Grand Island, New York, USA) was added after 45 h of culture to obtain a final concentration of 0.1 $\mu g \cdot mL^{-1}$ of Colcemid. All cultures were incubated at 37 °C. After incubation, cultures were centrifuged for 10 min 700 g and the supernatant was replaced by hypotonic solution (KCl 0.075 M, Gibco, Grand Island, New York, USA) prewarmed at 37 °C. After 10 minutes of treatment with the hypotonic solution at 37 °C cultures were centrifuged 5 min 700 ×g, and cells were fixed with methanol and acetic acid (3:1). For the cytogenetic analysis 2 to 3 days old slides were stained by the fluorescence plus Giemsa technique, using Hoechst 33258 stain in pH 6.8 phosphate buffer.

Chromosome analysis was carried out exclusively on first division metaphases containing 46 centromeres. The dicentric chromosomes (dic), tricentric chromosomes (tric), and centric rings (r) were only considered when their corresponding acentric fragment was present. Acentric fragments not related to a multicentric or a ring chromosome were recorded as extra acentric fragments (ace). For each irradiation condition, and following international criteria in cytogenetics dosimetry [34], the number of metaphases analyzed

was approximately 500, or those needed to score 100 chromosome aberrations. All metaphases with chromosome aberrations were analyzed independently by two scorers. During the analysis, the mitotic index was also calculated [34].

2.4. Statistical Analysis

To check if the distribution of chromosome aberrations after each irradiation condition followed a Poisson distribution, the dispersion index, variance/mean, and the normalized unit of this index, the U-test, were used [54]. Differences among irradiation conditions were evaluated by a one-way ANOVA test. Ordinary least squares method was used to calculate the linear regression between the dose and the frequency of chromosome aberrations.

3. Results

The average dose (±SD) of TLD measurements at 5, 10, 20 and 40 pulses are 0.12 (±0.02) Gy, 0.14 (±0.03) Gy, 0.22 (±0.06) Gy and 0.47 (±0.09) Gy respectively. From 5 to 10 pulses there was a slight non-significant increase in the mean dose, but from 10 to 40 pulses there was a linear increase in the mean dose (Figure 2). The slope of the linear regression indicates a mean of 12 mGy per pulse.

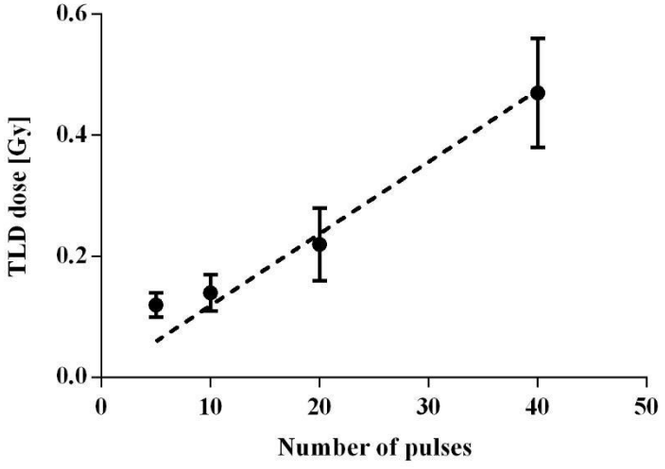

Figure 2. Mean dose measurement using TLD-100 in four irradiation conditions (5, 10, 20, and 40 pulses), bars represent standard deviation and broken lines represent linear fit.

Figure 3 shows microphotographs of representative metaphase for different X-rays pulsed conditions. Cytogenetic results are summarized in Table I. Eight out of 10 total irradiated samples could be analyzed to achieve ~ 500 cells or 100 dicentrics plus rings (40 pulses irradiation condition), and only in two cases, the number of cells analyzed was between 400 and 450 (at 5 and 20 pulses). The mitotic index was always higher than 2.5 %, which is considered a reference value in radiation cytogenetics [34]. In this work, the mitotic index seems not to be influenced by the number of X-rays pulses. One-way analysis of variance (ANOVA) is used to determine statistical significance differences between the chromosomal aberrations scoring on different exposure conditions, for dicentrics and extra acentric fragments, there was a clear increase as the number of pulses increased ($p< 0.0001$ in both cases). Significant differences were also observed for tricentric chromosomes obtained after 20 and 40 X-rays pulses ($p<0.0001$), and centric rings obtained for 5, 20, and 40 X-rays pulses ($p<0.0002$). The frequency of centric rings show a tendency to increase with the number of pulses. When total chromosome aberrations

were considered, there was a clear increase ($p < 0.001$). When the replicas were compared, similar frequencies of CA were observed. These results show the irradiation methodology and experimental setup of PF2kJ are robust.

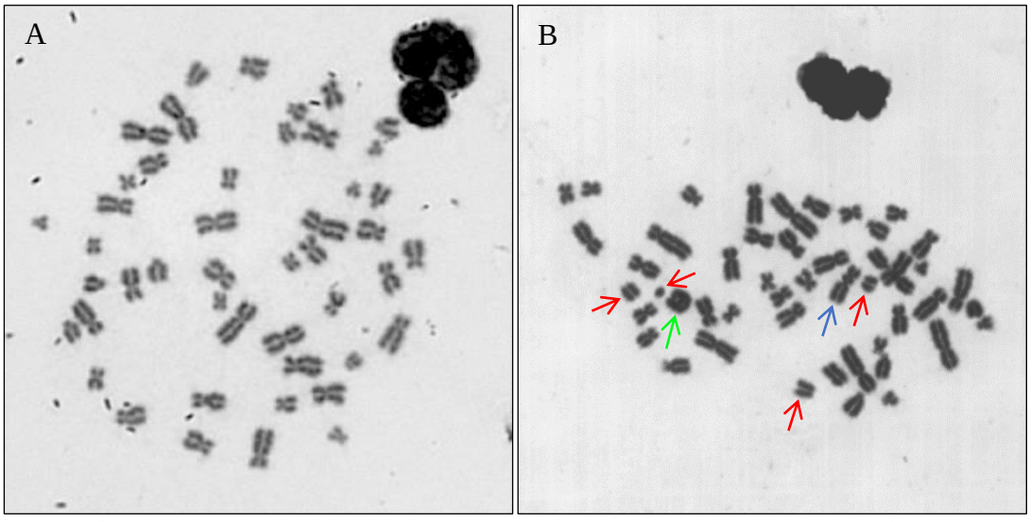

Figure 3. Metaphase observed after 0 pulses (A), and after exposure to 10 X-rays pulses (B). In B, the metaphase has one dicentric chromosome (blue arrow), one centric ring (green arrow), and four acentric fragments (red arrow).

Table I Cytogenetic results obtained from lymphocytes irradiated with X-rays pulses.

# pulses	MI	cells scored	dic	tric	r	ace	Total CA
0	10.6	500	0	0	0	0	0
0	10	500	0	0	0	0	0
5	6.3	411	9	0	3	2	14
5	5.4	500	12	0	2	4	18

10	10.7	500	27	0	0	21	48
10	9.5	500	25	0	2	16	43
20	8.2	500	78	0	12	33	123
20	5.1	433	77	3	7	39	126
40	10.2	217	93	1	6	56	156
40	8.2	225	91	1	7	50	149

MI: mitotic index; **dic**: dicentric chromosome; **tric**: tricentric chromosome; **r**: ring; **ace**: acentric fragment; **CA**: chromosome aberrations

Figure 4 shows the frequencies of different chromosome aberrations, calculated from the data in Table I, considering tricentrics as two dicentrics. As can be seen, for all types of CA there is a clear increase with dose. The linear coefficients (α) were 1.298 (± 0.153), 0.861 (± 0.106), 0.802 (± 0.094), and 0.443 (± 0.062) for Total CA, dic+r, dic, and ace respectively.

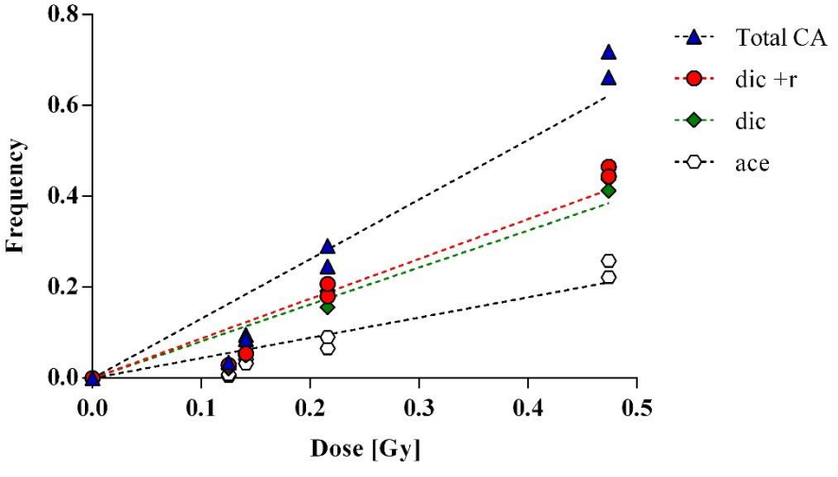

Figure 4. Dose dependence of chromosome aberrations in PBMCs irradiated by X-rays from PF-2kJ. Blue triangles represent the frequency of total chromosome aberrations (total CA); the red circles are dicentrics plus rings (dic+r); green diamond are dicentrics (dic); and white hexagon are acentric fragments (ace). Broken lines represent linear fit.

The chromosome aberrations frequency was calculated as the ratio of dicentrics plus rings and the total cells scored, Table II shows these results and dicentric plus ring cell distribution. After uniform exposure to low-LET radiation, dicentric cell distribution follows a Poisson distribution where the ratio between the variance and the mean, the dispersion index (DI) tends to 1, the DI is higher than 1 in all cases, indicating a tendency to show overdispersed values. This overdispersion was significant (U-test > 1.96) in one replica of each irradiation condition.

Table II. Intercellular distribution of dicentric chromosomes plus centric rings after X-rays pulses irradiation.

# pulses	cells scored	dic+r scored	dic+r distribution within cells						DI	U test
			0	1	2	3	4	5		

0	500	0	0	0	0	0	0	0	-	-
0	500	0	0	0	0	0	0	0	-	-
5	411	12	401	8	2	0	0	0	1.31	4.6
5	500	14	487	12	1	0	0	0	1.12	1.92
10	500	27	474	25	1	0	0	0	1.02	0.36
10	500	27	476	21	3	0	0	0	1.17	2.75
20	500	90	418	75	6	1	0	0	1.02	0.35
20	433	90	361	55	16	1	0	0	1.22	3.21
40	217	101	147	46	22	2	0	1	1.30	3.09
40	225	100	151	51	20	3	0	0	1.14	1.50

dic+r: dicentrics plus rings**; DI**: Dispersion index (σ^2/y)**; U test**; normalized unit of dispersion index, values >1.96 indicated overdispersion.

4. Discussion

The dicentric chromosomes and centric rings are two different kinds of unstable chromosome aberrations, they are specific to ionizing radiation with a clear dependence on dose, dose-rate and radiation quality. To the best of our knowledge, this work is the first study where cytogenetic biomarkers are analyzed in order to evaluate the biological effect of X-rays pulses at low doses (<0.5 Gy), ultra-high dose rate (107 Gy·s-1) and low energies (8-10 keV).

A monolayer of peripheral mononucleated cells (PBMCs) settled on the bottom of a Petri dish was used, in order to avoid a depth dose gradient in the irradiated sample due to the strong attenuation of such low photon energies. Additionally, the irradiation of unstimulated lymphocytes allows us to have all cells in the same phase of the cell cycle,

in this case in the G_0 quiescent stage. According to the irradiation conditions presented in [50, 55-58], to evaluate the induction of chromosome aberrations by conventional X-rays of low energies, some important factors have to be taking into account: i) a monolayer of cells, ii) cellular cycle control and iii) temperature control on irradiation assays. In the present study, petri dishes were kept at 37 °C before and just after irradiation, and although irradiations were not performed at 37 °C, they were above 17 °C as it is suggested by Gumrich et al. [59].

Previous studies have shown that higher doses of radiation result in an increased frequency of chromosome aberrations and a delay in cell cycle [51-53]. Consequently, the length of lymphocyte culture was set between 48-72 hours, depending on the number of pulses. All mitotic indexes were above 5 %, indicating that culture results were satisfactory. Because the cytogenetic analysis was restricted to first division metaphase, underestimation due to the analysis of second or third division metaphases was avoided.

Radiation exposures at ultra-high dose rates (10^6-10^7 Gy·s^{-1}, UHDRs) have been shown to manifest differential radiobiological responses, and induced less damage, compared to conventional (CONV) dose rates (0.001-0.4 Gy·s^{-1}) [5]. The increase in radical–radical recombination and oxygen depletion are the main hypotheses to explain a reduced yield of biological lesions at ultra-high dose rates [60]. Previous cytogenetic studies using UHDR have shown a decrease in the induction of chromosome aberrations when the number of pulses or the dose rate increased [61-63]. It should be noted that these earlier studies were performed in a higher energy range (in the order of MeV) and at higher radiation doses (2-8 Gy). In contrast, in the present study, we observed an increase in chromosome aberrations with the number of pulses. Our results seem to suggest that at low doses and for low-energy X-rays delivered at UHDR, there is a major biological effectiveness in producing DNA damage. Acharya et al. [63] observed an increase of

307 micronuclei yield when doses were delivered by multiple pulses compared with those
308 delivered by single pulse, especially at higher doses of 50 and 25 ns pulses. This seems
309 to indicate that for fractionation strategy short time of X-rays pulses (90 ns) which are
310 obtained from PF-2kJ, could be an important parameter on chromosome aberrations
311 induction.
312 Four reference dose-effect curves were applied to estimate the chromosome aberration
313 frequency expected at the physical doses reported in the present work (TLD-100): a α-
314 particle curve of ^{241}Am 2.7 MeV, 0.1 Gy·min^{-1} [55]; two X-rays curves, one of 180 kVp,
315 0.27 Gy·min^{-1} [64], and another of 10 keV, 0.5 Gy·min^{-1} [42]; and one γ radiation curve
316 of ^{60}Co, mean energy 1.25 MeV, 1.2-1.1 Gy·min^{-1} [65]. The frequencies values estimated
317 are shown in Figure 5, and compared with the frequency of dicentrics plus rings observed
318 in the present study. As it can be seen, the observed frequencies are higher than all the
319 frequencies that were estimated for the above indicated curves.
320
321

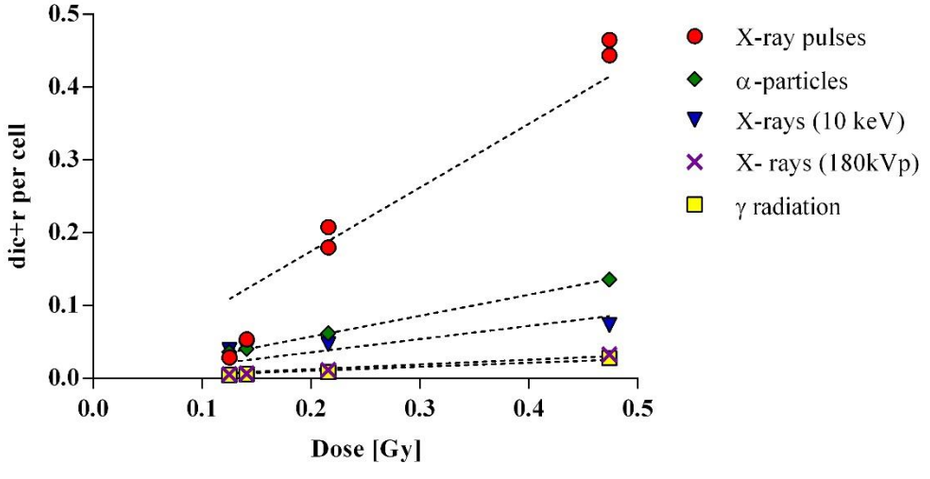

322

323 **Figure 5.** Comparison of dicentric plus rings (dic+r) frequency observed in the present
324 study (red circles), and frequencies calculated using previously published curves for α-

particles (green diamonds [55]), X-rays (blue invert triangle for 10 KeV [42]; and purple cross for 180 kVp [64]), and γ radiation (yellow squares [65]). Broken lines represent linear fit.

A weighted least-squares approximation was used to fit the data for each reference radiation quality. Considering irradiation conditions were performed at low doses values (< 0.5 Gy), and in order to compare the biological effect of X-rays pulses with conventional ionizing radiations sources, RBE_M was determined as the ratio α coefficient from linear fitting of the result reported in the present work, and α coefficient from linear fitting for reference radiations quality (α particles, X-rays and γ radiation). RBE_M values are shown in Table III, these results indicate that the photon energy of pulsed X-rays emitted by PF-2kJ is more effective compared even with high LET radiation.

Table III. Linear regression fit coefficient, and the biological relative effectiveness (RBE_M) for each type of radiation (α-particles, X-rays, γ-rays).

Radiation	**α**	**RBE_M**
Present data	0.875±0.079	-
α-particles[55]	0.288 ± 0.001	3.0
X-rays 10 keV[42]	0.181 ± 0.028	4.8
X-rays[64]	0.065± 0.004	13.5
γ-rays[65]	0.054 ± 0.004	16.2

α: linear coefficient; **RBE_M**: relative biological effectiveness.

In this study, the results show effects as those that are expected after high LET radiation exposures, indicating a different behavior of pulses radiation compared to conventional radiation. The intercellular distribution of dic+r showed a significant overdispersion at 5, 10, 20, and 40 pulses, where the u-test were 4.6, 2.75, 3.21, and 3.09 respectively. Since it is well known that for low-LET radiation dicentric and dicentric plus ring cell distribution agrees with the Poisson distribution, where the variance is equal to the mean. In the present study the overdispersion (variance > media) observed was unexpected. For these chromosome type aberrations overdispersion is expected after non-homogeneous exposure to low-LET radiation, or after high-LET radiation exposure. However, in this work we observed tricentric chromosomes, these multicentric configurations are rarely observed after low doses of low-LET exposure, and common after irradiations to low doses of high-LET [66-67].

Our results suggest that the pulsed X-rays of low-energy in low-dose range, with ultra-high dose rate interact distinctively with the DNA. Considering PF-2kJ has these characteristics it is necessary to gain a better understanding of mechanisms underlying the DNA damage induced by X-rays pulses such as by analyzing the formation of complex chromosome aberrations using fluorescence in situ hybridization (FISH) techniques, or evaluating the repair kinetics of the double strain break by analyzing the γ-H2AX foci [68]. The incorporation of others cytogenetic biomarkers could contribute to the characterization, since they allow direct evidence of the effects of radiations in biological systems.

5. Conclusions

In the present study our results evidence a different radiobiological response of PBMCs to pulsed irradiation. The presence of tricentrics and the overdispersion observed at low

doses, ultra-high dose rate and low energies of X-rays emitted by a PF-2kJ, suggest that the biological effect of X-rays pulses seems to be like high LET. The RBE_M analysis confirms this observation, where the pulses emitted by PF-2kJ are more effective inducing CA compared even with high LET radiation.

Acknowledgements

This work was financially supported by the ANID FONDECYT Regular project 1190677 Chile, the ANID FONDECYT Postdoctoral grant 3190184 Chile, and PIA Anillo ACT172101 grant Chile. The authors are thankful to the department of dosimetry of Chilean Nuclear Energy Commission for their support in the dose measurements.

Disclosure statement

No conflict of interest was reported by the authors.

References

1Jr M. C. Sauer, Sources of pulsed radiation, NATO Advanced Study Institutes Series, ASIC 86 (1981).

2R. A. Lewis, Journal of Physics D: Applied Physics, 47(37), 374001 (2014).

3R. J. Berry, E. J. Hall, D. W. Forster, T. H. Storr, and M. J. Goodman, J. Radiol. 42, 102 (1969).

4N. Esplen, M. S. Mendonca, and M. Bazalova-Carter, Physics in Medicine & Biology 65(23), 23TR03 (2020).

5A. A. Friedl, K. M. Prise, K. T. Butterworth, P. Montay-Gruel, and V. Favaudon, Med Phys. 49(3), 1993 (2022).

6J. Jain, H. Araya, J. Moreno, S. Davis, R. Andaur, B. Bora, C. Pavez, K. Marcelain and L. Soto, Journal of Applied Physics 130(16), 164902 (2021).

7J. Jain, J. Moreno, R. Andaur, R. Armisen, D. Morales, K. Marcelain, G. Avaria, B. Bora, S. Davis, C. Pavez et al., AIP Advances 7(8), 085121 (2017).

8F. Buontempo, E. Orsini, I. Zironi, L. Isolan, A. Cappellini, S. Rapino, A. Tartari, D. Mostacci, G. Cucchi, A. M. Martelli et al., PLoS One 13(6), e0199312 (2018).

9L. Isolan, D. Laghi, I. Zironi, M. Cremonesi, C. Garibaldi, F. Buontempo, and M. Sumini, Radiation Physics and Chemistry, 110296 (2022).

10Y. Kato and S. H. Be, Applied Physics Letters 48(11), 686 (1986).

11L. Soto, Plasma Physics and Controlled Fusion 47(5A), A361 (2005).

12N. K. Neog, S. R. Mohanty, and T. K. Borthakur, Physics Letters A 372(13), 2294 (2008).

13C. Pavez, J. Pedreros, M. Zambra, F. Veloso, J. Moreno, T. S. Ariel, and L. Soto, Plasma Physics and Controlled Fusion 54(10), 105018 (2012).

14J. Jain, J. Moreno, R. E. Avila, G. Avaria, C. Pavez, B. Bora, S. Davis, and L. Soto, In Journal of Physics: Conference Series 1043(1), 012048. IOP Publishing (2018).

15S. Auluck, P. Kubes, M. Paduch, M. J. Sadowski, V. I. Krauz, S. Lee, L. Soto, M. Scholz, R. Miklaszewski, H. Schmidt et al., Plasma 4(3), 450 (2021).

16T. Yamamoto, K. Shimoda, and K. Hirano, Japanese Journal of Applied Physics 24(3R), 324 (1985).

17M. Zakaullah, I. Akhtar, A. Waheed, K. Alamgir, A. Z. Shah, and G. Murtaza, Plasma Sources Science and Technology 7(2), 206 (1998).

18P. Silva, J. Moreno, L. Soto, L. Birstein, R. E. Mayer, and W. Kies, Applied Physics Letters 83(16), 3269 (2003).

19R. Niranjan, R. Srivastava, J. Joycee, and K. D. Joshi, Plasma Physics and Controlled Fusion 63(7), 075006 (2021).

20A. Bernard, H. Bruzzone, P. Choi, H. Chuaqui, V. Gribkov, J. Herrera, K. Hirano, A. Krejcí, S. Lee, C. Luo et al., Journal-Moscow Physical Society 8, 93 (1998).

21L. Jakubowski, M. Sadowski, and J. Zebrowski, Nuclear Fusion 41(6), 755 (2001).

22S. R. Mohanty, H. Bhuyan, N. K. Neog, R. K. Rout, and E. Hotta, Japanese Journal of Applied Physics 44(7R), 5199 (2005).

23J. Jain, J. Moreno, S. Davis, B. Bora, C. Pavez, G. Avaria, and L. Soto, Physics of Plasmas 26(10), 103105 (2019).

24J. Jain, J. Moreno, S. Davis, B. Bora, C. Pavez, G. Avaria, and L. Soto, Results in Physics 16, 102915 (2020).

25I. Escalona, G. Avaria, M. Díaz, J. Ardila-Rey, J. Moreno, C. Pavez, and L. Soto, Energies 10(9), 1415 (2017).

26G. Avaria, J. Ardila-Rey, S. Davis, L. Orellana, B. Cevallos, C. Pavez, and L. Soto, IEEE Access 7, 74899 (2019).

27L. Orellana, J. Ardila, G. Avaria, B. Cevallos, C. Pavez, R. Schurch, and L. Soto, In The International Symposium on High Voltage Engineering. Springer, Cham, 1367 (2019).

28A. Tarifeno-Saldivia and L. Soto, Physics of Plasmas 19(9), 092512 (2012).

29N. Talukdar, N. K. Neog, and T. K. Borthkur, Results in Physics 3, 142 (2013).

30J. Jain, J. Moreno, B. Bora, and L. Soto, Results in Physics 23, 104016 (2021).

31G. Obe and A. T. Natarajan, In: (Eds.) Chromosome Aberrations; Karger: Basel, Switzerland (2004).

32P. E. Bryant, Heidelberg, Germany: Springer, 178 (2007).

33E. A. Ainsbury, E. Bakhanova, J. F. Barquinero, M. Brai, V. Chumak, V. Correcher, F. Darroudi, P. Fattibene, G. Gruel, I. Guclu, et al., Radiat Prot Dosimetry 147(4), 573 (2011).

34IAEA, Vienna (Austria): EPR Biodosimetry, International Atomic Energy Agency (2011).

35H. Romm, U. Oestreicher, and U. Kulka, Ann Ist Super Sanita 45(3), 25 (2009).

480 36U. Oestreicher, D. Samaga, E. A. Ainsbury, A. C. Antunes, A. Baeyens, L. Barrios, C.
481 Beinke, P. Beukes, W. F. Blakely, A. Cucu et al., Int J Radiat Biol. 93(1), 20 (2017).
482
483 37M. A. Hill, Radiation Protection Dosimetry 112(4), 471 (2004).
484
485 38ICRP, ICRP Publication 92. Ann. ICRP 33 (4) (2003).
486
487 39E. Schmid, D. Regulla, S. Guldbakke, D. Schlegel, and M. Roos, Radiation Research
488 157(4), 453 (2002).
489
490 40E. Schmid, D. Regulla, H. M. Kramer, and D. Harder, Radiation Research 158(6), 771
491 (2002).
492
493 41L. C. Paterson, A. Yonkeu, F. Ali, N. D. Priest, D. R. Boreham, C. B. Seymour, F.
494 Norton, and R. B. Richardson, Radiat Res. 195(2), 211 (2020).
495
496 42M. Krumrey, G. Ulm, and E. Schmid, Radiat Environ Biophys. 43(1), 1 (2004).
497
498 43N. Hunter and C. R. Muirhead, Journal of Radiological Protection: Official Journal of
499 the Society for Radiological Protection 29(1), 5 (2009).
500
501 44C. Pavez, M. Zorondo, J. Pedreros, A. Sepúlveda, L. Soto, G. Avaria, J. Moreno, S.
502 Davis, B. Bora and J. Jain, Plasma Physics and Controlled Fusion 65(1), 015003 (2022).
503

504 45B. Obryk, C. Hranitzky, H. Stadtmann, M. Budzanowski, and P. Olko, Radiation
505 Protection Dosimetry 144, No. 1–4, 211 (2011).
506
507 46L. G. Massillon-J, A. Cabrera-Santiago, R. Minniti, M. O'Brien, and C. G. Soares,
508 Physics in Medicine & Biology 59 (15) (2014).
509
510 47J. M. Ixquiac-Cabrera, M. E. Brandan, A. Martínez-Dávalos, M. Rodríguez-Villafuerte,
511 C. Ruiz-Trejo, and I. Gamboa-deBuen, Radiation Measurements 46 (4), 389 (2011).
512
513 48V. Dubrovsky, I. G. Gazaryan, V. A. Gribkov, Y. P. Ivanov, O. A. Kost, M. A. Orlova,
514 and N. N. Troshina, Journal of Russian Laser Research 24(4), 289 (2003).
515
516 49D. Díaz, Master's thesis, Physics Institute: Pontificia Universidad Católica de Chile
517 (2018).
518
519 50R. P. Virsik, C. Schäfer, D. Harder, D. T. Goodhead, R. Cox, and J. Thacker, Int J Radiat
520 Biol Relat Stud Phys Chem Med. 38(5), 545 (1980).
521
522 51D. C. Lloyd, G. W. Dolphin, R. J. Purrott, and P. A. Tipper, Mutat Res. 42,401 (1977).
523
524 52E. Gudowska-Nowak, A. Kleczkowski, E. Nasonova, M. Scholz, and S. Ritter,
525 International Journal of Radiation Biology 81(1), 23 (2005).
526
527 53A. Heimers, H. J. Brede, U. Giesen, and W. Hoffmann, Radiat Environ Biophys. 44(3),
528 211 (2005).

54D. G. Papworth, Radiat. Bot. 15, 127 (1975).

55E. Schmid, L. Hieber, U. Heinzmann, H. Roos, and A. M. Kellerer, Radiat Environ Biophys. 35(3), 179 (1996).

56T. E. Schmid, U. Oestreicher, M. Molls, and E. Schmid, Radiat Res. 176(2), 226 (2011).

57M. S. Sasaki, In: Fielden, E.M., O'Neill, P. (eds) The Early Effects of Radiation on DNA. NATO ASI Series. 54. Springer, Berlin, Heidelberg (1991).

58H. Roos and E. Schmid, Radiat Environ Biophys. 36(4), 251 (1998).

59K. Gumrich, R. P. Virsik-Peuckert, and D. Harder, Int J Radiat Biol Relat Stud Phys Chem Med. 49(4), 665 (1986).

60V. Favaudon, R. Labarbe, and C. L. Limoli, Med Phys. 49(3), 2068 (2022).

61T. Prempree, A. Michelsen, and T. Merz, Int J Radiat Biol Relat Stud Phys Chem Med. 15(6), 571 (1969).

62R. J. Purrott and E. J. Reeder, Int J Radiat Biol Relat Stud Phys Chem Med. 31(3), 251 (1977).

553 63S. Acharya, N. N. Bhat, P. Joseph, G. Sanjeev, B. Sreedevi, and Y. Narayana, Radiat
554 Environ Biophys. 50(2), 253 (2011).
555
556 64J. F. Barquinero, L. Barrios, M. R. Caballín, R. Miró, M. Ribas, and J. Egozcue, Int J
557 Radiat Biol. 71(4), 435 (1997).
558
559 65J. F. Barquinero, L. Barrios, M. R. Caballín, R. Miró, M. Ribas, A. Subias, and J.
560 Egozcue, Mutat Res. 326(1), 65 (1995).
561
562 66R. M. Anderson, S. J. Marsden, E. G. Wright, M. A. Kadhim, D. T. Goodhead, and C.
563 S. Griffin, Int J Radiat Biol. 76(1), 31 (2000).
564
565 67J. F. Barquinero, G. Stephan, and E. Schmid, Int J Radiat Biol. 80(2), 155 (2004).
566
567 68M. Borràs-Fresneda, J. F. Barquinero, M. Gomolka, S. Hornhardt, U. Rössler, G.
568 Armengol, and L. Barrios, Sci Rep 6(1), 1 (2016).

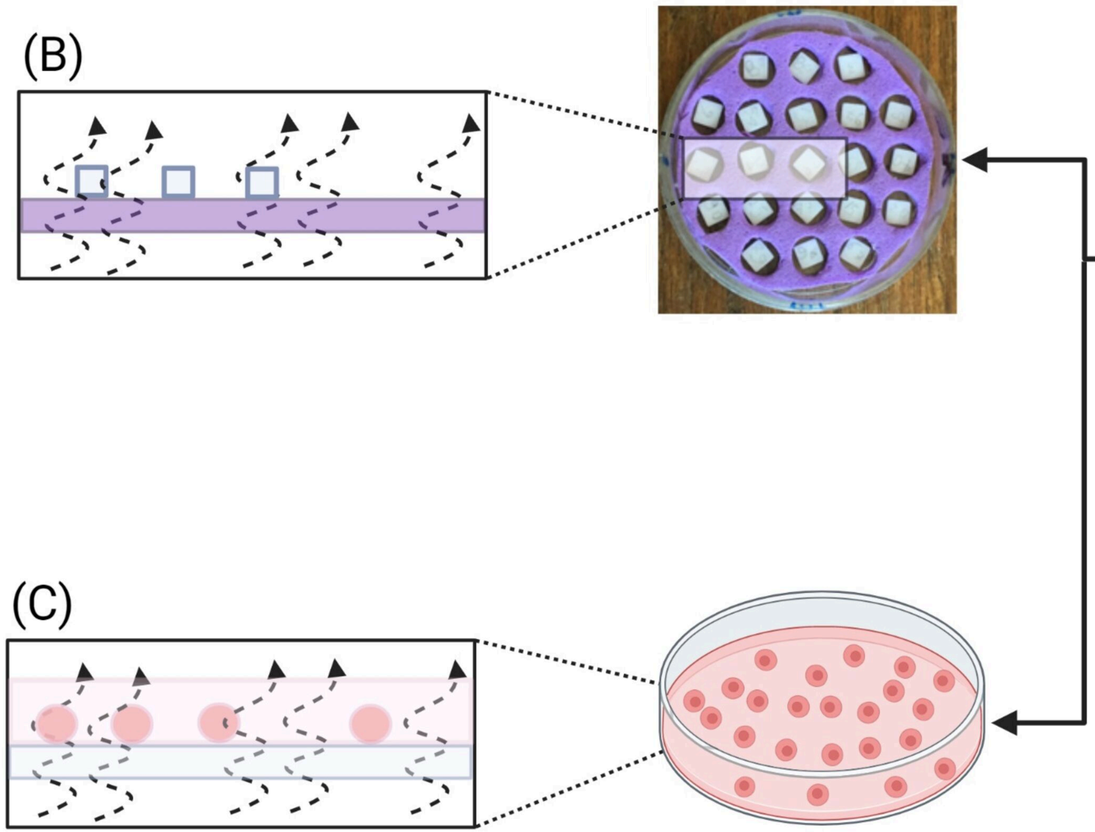

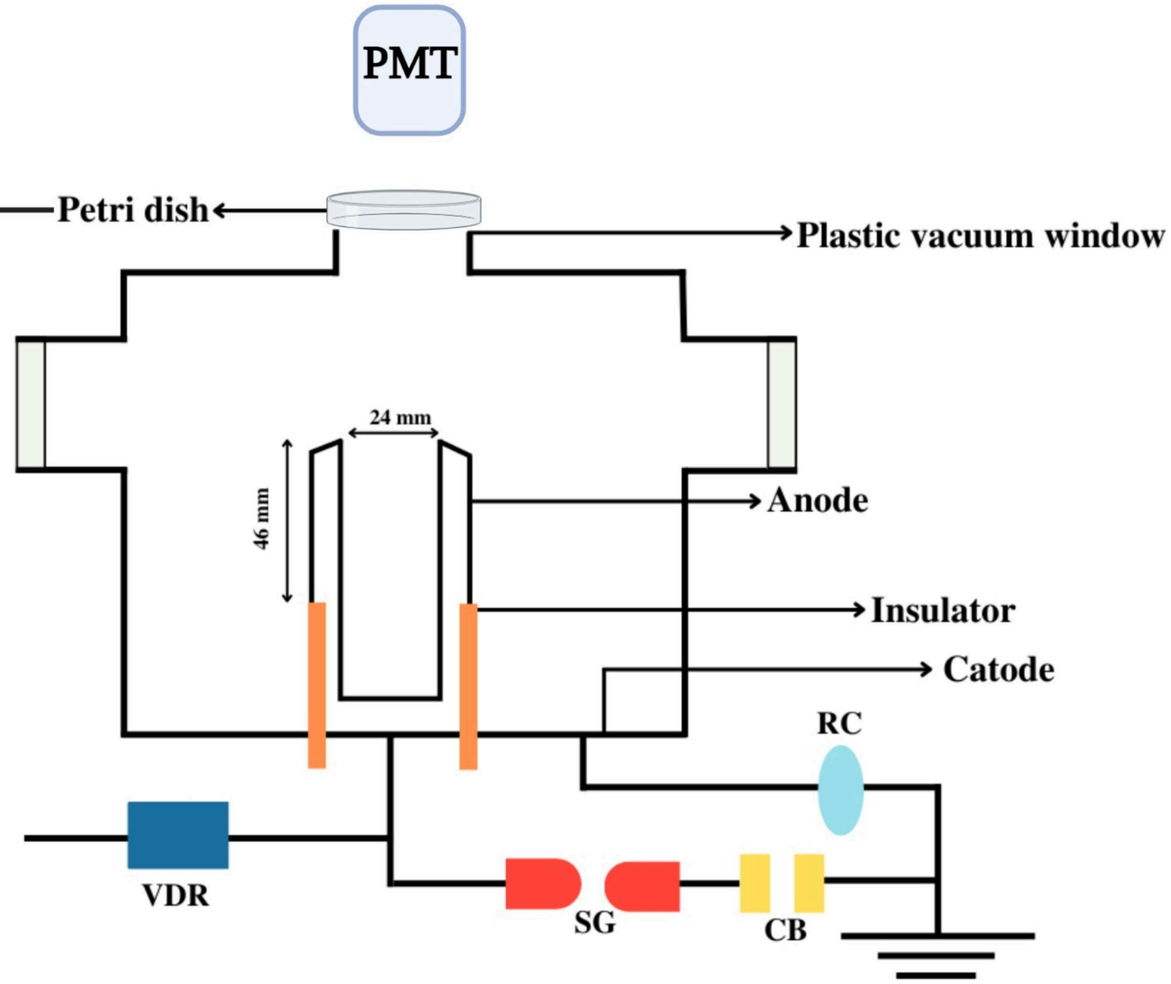

(A)

AIP Publishing

Journal of Applied Physics

ACCEPTED MANUSCRIPT

PLEASE CITE THIS ARTICLE AS DOI: 10.1063/5.0141529

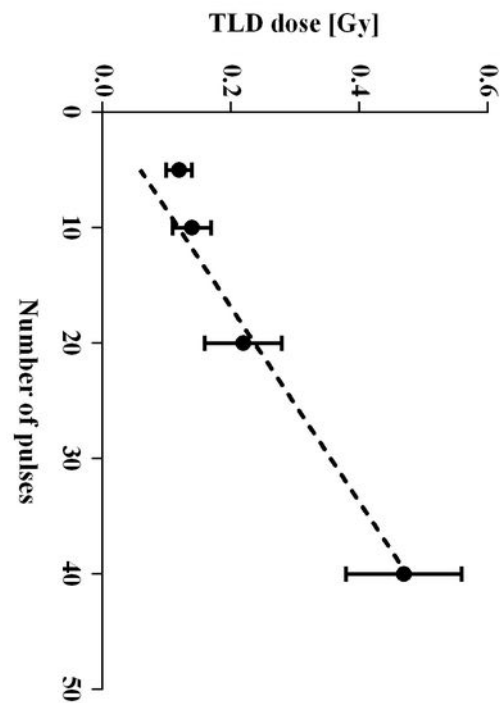

AIP Publishing

Journal of Applied Physics

ACCEPTED MANUSCRIPT

PLEASE CITE THIS ARTICLE AS DOI: 10.1063/5.0141529

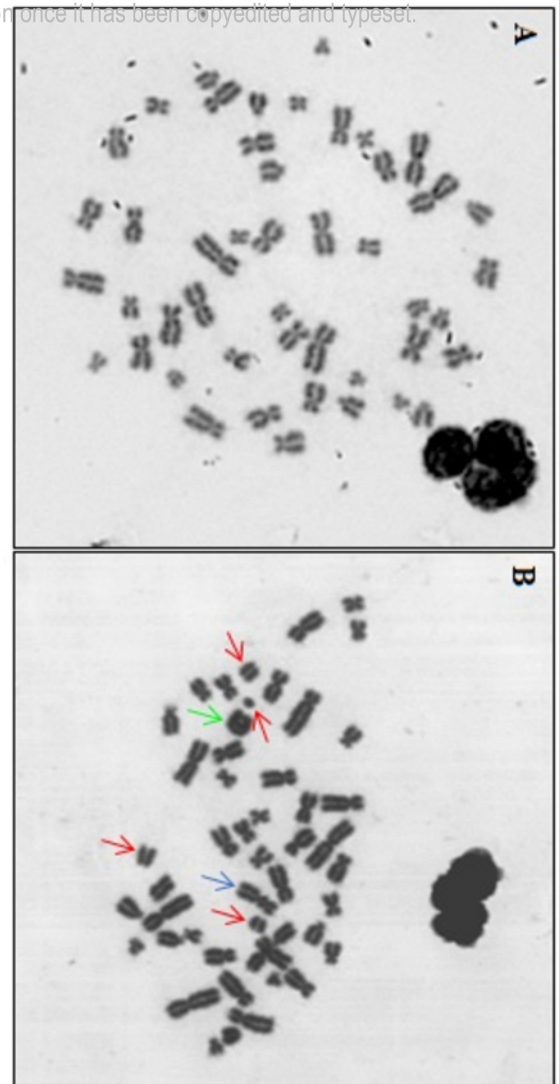

AIP Publishing

Journal of Applied Physics

ACCEPTED MANUSCRIPT

PLEASE CITE THIS ARTICLE AS DOI: 10.1063/5.0141529

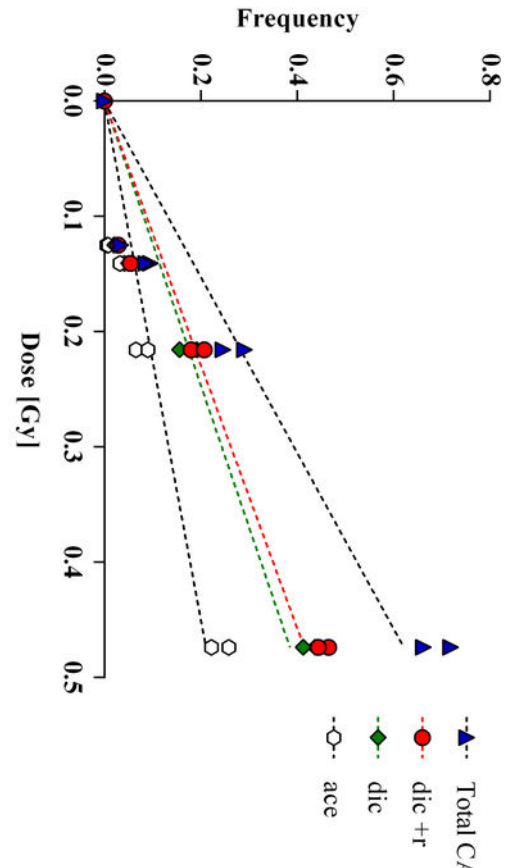

AIP Publishing

Journal of Applied Physics

ACCEPTED MANUSCRIPT

PLEASE CITE THIS ARTICLE AS DOI: 10.1063/5.0141529